# Vibronic spectroscopy of jet-cooled indazole: $S_1 \leftrightarrow S_0$ spectra and mode assignments

Erko Jalviste[a] and F. Temps[b]
*Institut für Physikalische Chemie, Universität Kiel, Olshausenstr. 40, D-24098 Kiel, Germany*

(Received 11 February 1999; accepted 26 May 1999)

The $S_0 \leftrightarrow S_1$ electronic transition of 1H-indazole has been investigated by laser-induced fluorescence (LIF) excitation and dispersed fluorescence (DF) spectroscopies in a supersonic free jet expansion. Ground and excited state vibrational modes were assigned based on the observed band frequencies and intensities, *ab-initio* frequency calculations, and available infrared absorption data. Unexpected ''symmetry forbidden'' transitions were observed in the DF, which, according to our assignments, would originate from the $27^1$ excited state in-plane fundamental to several ground state out-of-plane fundamentals. Accepting the assignments, this observation would indicate a vibronic coupling between the $S_1$ (or $S_0$) state ($A'$) and an excited $n\pi^*$-type electronic state of $A''$ symmetry. © *1999 American Institute of Physics.* [S0021-9606(99)00332-3]

## I. INTRODUCTION

Indazole is an enticing molecule because of its two tautomeric forms, 1H-indazole and 2H-indazole (Fig. 1), which are distinguished by the position of the H atom. However, compared to other bicyclic heteroaromatic molecules, rather little is known about its vibrational structure. This structure is of fundamental interest for understanding tautomerization dynamics.

Considering previous work, the electronic absorption spectrum of the indazole solution has been measured by Schütt and Zimmermann.[1] They assigned the molecule's first three excited electronic states observed at ≈33 600, 38 510, and 48 000 $cm^{-1}$ to $^1L_b$, $^1L_a$, and $^1B_b$, respectively. The UV absorption spectrum of indazole vapor was later reported by Byrne and Ross.[2] Subsequently, a microwave study performed by Velino *et al.*[3] yielded precise ground state rotational constants for the molecule. A vibrational analysis based on infrared and Raman measurements of polycrystalline indazole, oriented single crystals, and indazole solution has been reported by Bigotto and Zerbo.[4] At about the same time, the infrared absorption spectrum of indazole vapor has been investigated by Cané *et al.*[5] The same group also analyzed the band contour of the $S_1 \leftarrow S_0$ electronic origin transition at ≈300 nm and determined approximate excited state rotational constants.[6] The precision of these excited state rotational constants and the frequency of the electronic origin transition (34 471.69 $cm^{-1}$) were greatly improved by a recent analysis of rotationally resolved $S_1(^1L_b) \leftarrow S_0$ laser-induced fluorescence (LIF) excitation spectra measured in a molecular beam by Berden *et al.*[7] This work also yielded the transition dipole moment angle (62.2°) and the axis switching angle (1°). Eventually, the relative stability of the 1H- and 2H-indazole tautomers in the ground electronic state has been examined by *ab-initio* calculations in the work of Catalan *et al.*[8] These authors also compared the solution absorption spectra of indazole and its 1-methyl and 2-methyl derivatives. They predicted 1H-indazole to be more stable than 2H-indazole by ≈3.6 kcal/mol (≈1300 $cm^{-1}$).

In all studies reported above only the 1H-indazole tautomer was observed. This was confirmed by the values of the ground state rotational constants from the microwave[3] and from the high resolution electronic[7] spectra. To the best of our knowledge, no experimental evidence is available about the 2H-tautomer.

The successful analysis of jet-cooled vibronic spectra of related molecules, for example indole,[9] benzimidazole,[10] and benzotriazole,[10,11] motivated us to initiate a detailed study of the vibrational structure and dynamics of indazole (i.e., 1H-indazole). The aim is eventually to explore the tautomerization dynamics (1,2-H atom shift) in indazole and complexes of indazole in the ground electronic state. For this relatively large aromatic molecule, only a combined analysis of data from electronic spectra, infrared spectra, and modern *ab-initio* calculations can provide a way for detangling the vibrational structures of the ground and excited electronic states. Thus, in the present paper, we report on our results of a vibrational analysis of the $S_1(^1L_b) \leftrightarrow S_0$ electronic spectrum of 1H-indazole. The investigations, which we carried out by using LIF excitation and dispersed fluorescence (DF) spectroscopies and by employing *ab-initio* calculations, allowed us to derive assignments for the ground state normal mode vibrations and for many excited electronic state vibrations. The knowledge of the vibrational modes will be helpful for studying indazole as a test case for a unimolecular 1,2 proton transfer reaction in the electronic ground state at different levels of vibrational excitation. Spectra of indazole–water complexes[12] will be considered in a separate publication.

## II. EXPERIMENT

A supersonic free jet was formed by the expansion of He gas containing a trace amount of indazole vapor through the

[a]Permanent address: Institute of Physics, Tartu University, Riia 142, 51014 Tartu, Estonia.
[b]Electronic mail: temps@phc.uni-kiel.de

 

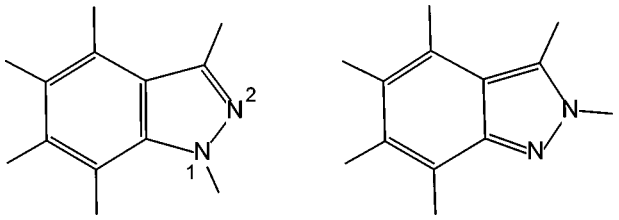


FIG. 1. The tautomeric forms of 1H-indazole and 2H-indazole. Atom numberings are indicated for the N atoms.

0.8 mm orifice of a heatable pulsed valve (General Valve #9) into a vacuum chamber. The indazole sample was kept in a small reservoir heated to ≈150° in the He supply line. Optimal backing pressures were of the order of ≈6 bar. The chamber was evacuated with a roots pump (Alcatel RSV 601) backed by a rotary pump. Practically collision-free conditions were ensured in the jet expansion during the short (≈30 ns) excited state indazole lifetime.[7]

The unfocused beam from a Nd:YAG pumped pulsed dye laser (Continuum 661 and Spectra Physics PDL-3, 20 Hz pulse repetition rate) with an external BBO frequency doubling crystal (Lambda-Physik FL 37.3) was used for the LIF excitation. Fluoresceine 548, Rh6G, RhB, or a mixture of Rh6G and RhB dyes dissolved in methanol were used to cover the wavelength region from 305 to 272 nm. Fluorescence was collected perpendicular to the jet axis and the excitation beam and focused onto a photomultiplier tube (PMT) or, for the DF measurements, onto the entrance slit of a monochromator. The signal from the PMT was fed to a boxcar integrator (Stanford Research) and stored on a PC microcomputer via a GPIB interface. One recorded data point was the average of 25 laser pulses.

For the LIF excitation measurements, the distance between the nozzle orifice and the excitation laser beam was ≈1.5 cm. The dye laser scan speed was typically $2.3\times10^{-3}$ nm/s (in the UV). The known electronic origin frequency of 34 471.7 $cm^{-1}$ from the high resolution spectrum[7] was used for absolute wavelength calibration.

For the DF measurements, the fluorescence light was dispersed using an 0.75 m, $f/6$ monochromator (SPEX 750M) with a 1200 lines/mm grating. The UV beam crossed the jet 0.5 cm downstream from the nozzle orifice. DF spectra were initially recorded in the traditional grating scan mode, with a scan speed of typically 0.01 nm/s, using a PMT detector behind the monochromator exit slit. The slit widths were typically set to 0.05 mm, resulting in a resolution of ≈8 $cm^{-1}$. Wavelength markers generated by the monochromator control program were recorded simultaneously with the spectrum. For stronger excitation bands the intensity of the resonance band was determined by subtracting the scattered laser light measured without the gas pulse. In later experiments, the PMT was replaced by an image intensified gated CCD camera (Princeton Instruments ICCD-576G1). The CCD array had 576×384 pixels. The excitation frequency (laser setting) and the known total CCD coverage range of 14.057(2) nm were used for wavelength calibration. The CCD range was determined by measuring the known emission lines of Ne between 330 and 380 nm from a discharge lamp. With a monochromator entrance slit width of 0.025 mm, the resolution was ≈10 $cm^{-1}$ (corresponding to ≈3.5 pixels). A further reduction of the slit width did not improve the resolution significantly.

## III. RESULTS

1H-indazole is a planar molecule of $C_s$ symmetry. The planarity in both the ground and excited state was confirmed by the small inertial defect calculated from the rotational constants.[3,7] The molecule's 15 atoms give rise to 39 normal modes, including 27 in-plane (totally symmetric, $A'$) vibrations and 12 out-of-plane ($A''$) vibrations. The vibronic (electronic-vibrational) selection rules for the $S_1\leftrightarrow S_0$ transition ($\pi\pi^*$), governed by an in-plane transition dipole moment, are $A'\leftrightarrow A'$, $A''\leftrightarrow A''$. Hence, since both electronic states are of $A'$ symmetry, the vibrational selection rules (within the Condon approximation) are, likewise, $A'\leftrightarrow A'$, $A''\leftrightarrow A''$. The $S_0$ and $S_1$ vibrational modes are numbered in the following according to their calculated *ab-initio* frequencies.

### A. Assignment procedure

Assigning the observed $S_1\leftrightarrow S_0$ spectra implies identification of the observed LIF excitation and DF bands in terms of the respective $S_0$ and $S_1$ normal mode vibrations and determination of the compositions of these bands in terms of respective quantum numbers for the $S_0$ and $S_1$ states. Spectra were assigned by considering (i) the observed band frequencies and their intensities in the excitation and in the DF spectra of this work; (ii) the calculated *ab-initio* frequencies of this work; (iii) the reported experimental gas phase infrared absorption frequencies and intensities of Cané *et al.*;[5] and (iv) in a few cases also the calculated infrared intensities of the fundamentals.

A critical step of the procedure was to establish the correspondence between the upper state and ground state fundamentals. This was mostly based upon the identification of the strongest bands in the $\Delta v=0$ regions in the DF spectra. It was presumed that the vibrational modes, of which the observed bands were composed, retained most of their character upon the transition between the two electronic states. We denote corresponding modes below as respective $S_0$ and $S_1$ ''pairs'' or ''counterparts.'' Combination differences between the fundamentals, their overtones, and respective combination bands could then be used to check initial ''trial'' assignments and propose new assignments.

### B. *Ab-initio* calculations

*Ab-initio* calculations were carried out with the GAUSSIAN-94 package.[13] Geometry optimizations were performed at the MP2/6-31G* level for the $S_0$ state and at the CIS/6-31G* level for the $S_1$ state. The optimizations without planarity constraints resulted in planar structures for both $S_0$ and $S_1$. Optimized MP2/6-31G* and CIS/6-31G* geometries were subsequently used for the calculations of the frequencies and the shapes of the respective normal modes. Schematic representations of the calculated $S_0$ and $S_1$ state

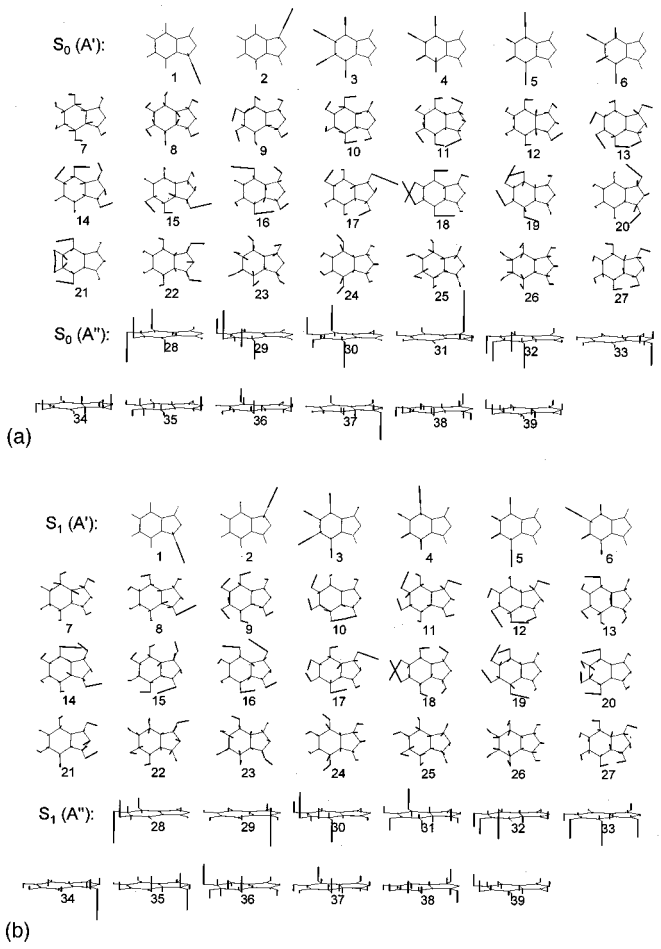


FIG. 2. Calculated normal mode vibrations of 1H-indazole. (a) $S_0$ state vibrations at the MP2/6-31G* level of theory; (b) $S_1$ state vibrations at the CIS/6-31G* level of theory. The position of the N atoms are the same as in Fig. 1.

normal modes (Cartesian atomic displacements) are presented in Fig. 2.

It is realized that *ab-initio* computations at the CIS level on aromatic systems typically overestimate the transition energies to the $L_b$ and $L_a$ states. The problem arises that the error may be greater for $L_b$, which requires more doubly excited configurations for its description than $L_a$. As a result, there can be a situation that the two lowest electronic states ($S_1$ and $S_2$) are computed in opposite (i.e., wrong) order.[14] CIS optimizations were therefore run also for the $S_2$ state. Since for indazole the observed $S_2-S_1$ spacing ($\approx 5000\,\mathrm{cm}^{-1}$, Ref. 1) and the calculated $S_2-S_1$ spacing ($\approx 4000\,\mathrm{cm}^{-1}$) turned out relatively large, it was concluded that the lowest calculated excited state does indeed most likely correspond to the observed $S_1$ state. Further support for this conclusion was drawn from the observations that (i) the differences of the computed $S_1$ and $S_0$ rotational constants were closer to the measured values[7] than the corresponding computed $S_2$ and $S_0$ differences, and that (ii) the measured axis switching angle ($+1.0°$, Ref. 7) is in much better agreement with the calculated angle for the $S_1 \leftarrow S_0$ transition ($+1.1°$) rather than with that calculated for the $S_2 \leftarrow S_0$ transition ($-0.9°$). Rotational constants and axis switching angles were obtained from the CIS/3-21G geometry for the $S_1$ state, the CIS/3-21G geometry for the $S_2$ state, and the HF/3-21G geometry for the $S_0$ state.

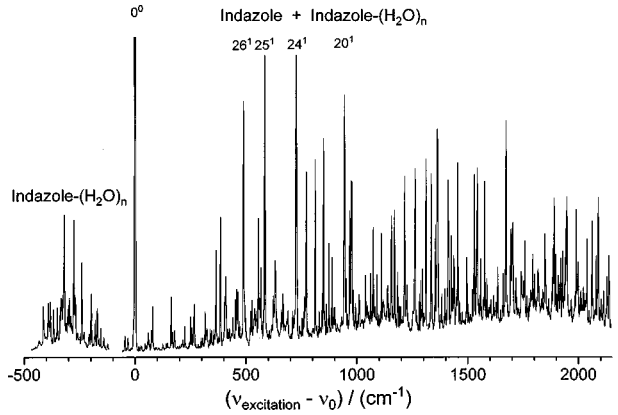


FIG. 3. Overview of the $S_1 \leftarrow S_0$ LIF excitation spectrum of jet-cooled indazole. The spectral range shown was covered using four different dye mixtures. Intensities have not been normalized in this scan for pump power variations over the dye laser tuning curves. The spectrum that was measured just after loading a fresh indazole sample also shows excitation bands of indazole–water complexes (see the text). An expanded part of the spectrum with vibrational assignments is shown in Fig. 4.

With these premises, the observed vibrations were correlated with the calculated ones in most cases in the order of the frequencies, with the assumption that the ratio between the observed and the calculated frequencies was approximately uniform. Some exceptions will be mentioned separately. Useful additional information was obtained from calculated MP2/6-31G* IR absorption intensities. With an average deviation of a factor of 0.97 (observed/calculated), the calculated $S_0$ frequencies matched the experimental ones very nicely. As one may expect, however, the deviations for the $S_1$ state were larger (0.91). Hence, while observed $S_0$ vibrational levels could usually be identified based on the comparison with the *ab-initio* data, $S_1$ mode assignments could be deduced only after a detailed examination of all data, including especially the mode frequency and intensity information from the DF spectra.

### C. The $S_1 \leftarrow S_0$ LIF excitation spectrum

An overview of the $S_1 \leftarrow S_0$ LIF excitation spectrum of indazole is presented in Fig. 3. The spectrum that has been composed from four scans measured with different laser dyes (not normalized for variations of laser power) illustrates the very complicated vibrational structure of the molecule. As seen, the electronic origin band of the free indazole molecule was the strongest feature in the excitation spectrum. This implicates a rather small geometry change upon the electronic transition. Nevertheless, the Franck–Condon range was found to extend for several $1000\,\mathrm{cm}^{-1}$ toward the blue of the origin (only a portion of the spectrum has been reproduced in Fig. 3). Bands seen to the red of the origin of the free indazole molecule were attributed to indazole–water complexes. The spectrum in Fig. 3 was taken with a fresh sample of indazole and the indazole–water complexes appeared because some water was present as an impurity in the

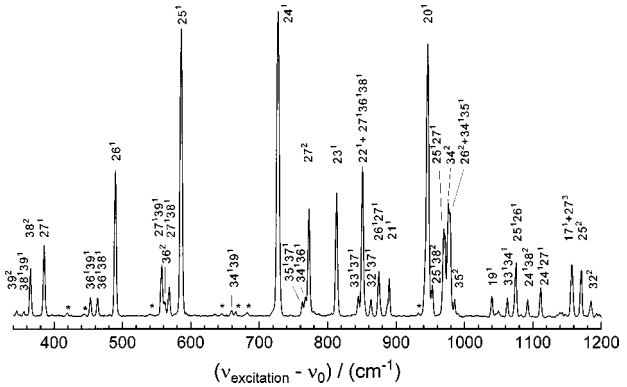


FIG. 4. An expanded portion of the LIF excitation spectrum of jet-cooled indazole of Fig. 3 from 350–1200 cm$^{-1}$ above the $0_0^0$ origin band at $\nu(0_0^0) = 34\,471.7$ cm$^{-1}$. Spectral resolution: $\approx 3$ cm$^{-1}$. Bands of indazole–water clusters are marked by asterisks.

fresh sample. After several days of operation without replacing the sample, the bands of the complexes were significantly smaller (see Fig. 4 for comparison). Bands of the complexes were found in the entire excitation spectrum, but they were usually weaker toward the blue of the free indazole origin. Excitation bands belonging to the complexes were identified also by their characteristic DF spectra (below). An expanded part of the LIF excitation spectrum from the indazole origin toward the blue is presented in Fig. 4. The linewidths seen in this spectrum were determined by the rotational band contours ($\approx 3$ cm$^{-1}$). A notable observation was the apparent absence of strong ''hot band'' excitation transitions originating from vibrationally excited $S_0$ levels, although contributions of some weak hot bands were not ruled out.

The observed $S_1$ vibrational term energies with their assignments are given in Table I. These assignments were derived with the DF spectra from the respective $S_1$ terms (below) and with the *ab-initio* calculations. It is useful to summarize some main points here, before considering the DF spectra in detail in the following section:

(i) The strongest excitation bands in Fig. 4 were expected to lead to in-plane fundamentals in the $S_1$ state. Accordingly, the bands observed with the highest intensities (second to the origin band) were assigned to $25^1$, $24^1$, and $20^1$. Furthermore, modes $\nu_{27}$, $\nu_{26}$, and $\nu_{25}$ were found to stand out because of easily assignable overtone bands ($27^2$, $26^2$, and $25^2$) and $\nu_{26}$, $\nu_{25}$, and $\nu_{24}$ were observed in combination with $\nu_{27}$ ($26^127^1$, $25^127^1$, and $24^127^1$).

(ii) Considerable activity was also detected of certain two quantum overtones and combinations of $S_1$ out-of-plane modes. Excitation bands of this kind were seen, for example, to lead to $38^2$, $36^139^1$, and $36^138^1$. These $S_1$ two quantum out-of-plane mode combination levels are of $A'$ symmetry. The observed bands were therefore symmetry allowed, although they were, in general, weaker and hence more difficult to assign (see below).

(iii) The calculated normal mode shapes (Fig. 2) helped to identify corresponding ''pairs'' of $S_1$ and $S_0$ modes (in the sense described above) in some ambiguous cases because strong bands in the DF spectra could be qualitatively predicted.

TABLE I. Vibrational band positions in the measured 1 H-indazole $S_0 \leftarrow S_1$ LIF excitation spectrum and corresponding $S_1$ state vibrational assignments. All assigned bands originate from the $0_0$ vibrational ground state. Band frequencies are given with respect to the $0_0^0$ origin band at 34 471.69 cm$^{-1}$. Assignments of the corresponding $S_0$ counterparts of the $S_1$ excited modes were made by reference to the strongest band(s) in the $\nu = 1 \rightarrow \nu' = 1$ region of the DF spectra observed after excitation of the respective $S_1$ levels.

| Frequency (cm$^{-1}$) | Intensity | $S_1$ assignment | $S_0$ counterpart |
|---|---|---|---|
| +0.00 | vs | $0^0$ | $0_0$ |
| +345 | vw | $39^2$ | $39_2$ |
| +355 | vw | $38^139^1$ | $38_139_1$ |
| +364 | m | $38^2$ | $38_2$ |
| +385 | m | $27^1$ | $27_1$ |
| +453 | w | $36^139^1$ | $35_139_1$ |
| +463 | w | $36^138^1$ | $35_138_1$ |
| +489 | s | $26^1$ | $26_1$ |
| +557 | m | $27^139^1$ | $34_139_1$ |
| +562 | w | $36^2$ | $35_2$ |
| +568 | m | $27^138^1$ | $34_138_1$ |
| +586 | vs | $25^1$ | $25_1$ |
| +659 | vw | $34^139^1$ | $33_139_1$ |
| +727 | vs | $24^1$ | $24_1$ |
| +763 | w | $35^137^{1a}$ | $36_137_1$ |
| +767 | w | $34^136^1$ | $33_135_1$ |
| +772 | s | $27^2$ | $34_2$ |
| +813 | s | $23^1$ | $22_1$ |
| +844 | w | $33^137^{1b}$ | $32_138_1$, #[c] |
| +851 | s | $22^1+27^136^138^1$ | $23_1+33_138_1$, $20_1$, $37_2$ |
| +863 | w | $32^137^1$ | $34_1$, $36_1$ |
| +874 | m | $26^127^1$ | $26_127_1$ |
| +889 | m | $21^1$ | $23_1+33_138_1$ |
| +946 | vs | $20^1$ | $21_1+$#[c] |
| +951 | m | $25^138^2$ | $26_138_2+$?[d] |
| +971[e] | s | $25^127^1$ | $25_127_1$ |
| +976 | s | $34^2$ | $33_2+32_134_1$ |
| +978 | s | $26^2+34^135^1+32^127^1$ | $26_2$, $37_2$ |
| +985 | w | $35^2$ | $13_1$, $12_1$, ?[f] |
| +991 | vw | $30^138^1$ | $29_138_2$ |
| +1040 | w | $19^1$ | $19_1$ |
| +1062 | w | $33^134^1$ | $32_133_1$ |
| +1076 | m | $25^126^1$ | $25_126_1$ |
| +1092 | w | $24^138^2$ | $24_138_2$ |
| +1111 | m | $24^127^1$ | $24_127_1$ |
| +1157[e] | m | $17^1+27^3$ | $17_1$ |
| +1171 | m | $25^2$ | $25_2$ |
| +1185[e] | w | $32^2$ | $32_2$, ?[f] |
| +1216 | m | $24^126^1$ | $24_126_1$ |
| +1263 | w | $15^1$ | $15_1$ |

[a]An alternative assignment for this band is $32^139^1$.

[b]An alternate assignment for this band is $26^138^139^1$, which corresponds to the $26_138_139_1$ level in the $S_0$ state.

[c]The # marks an unassigned band at 1000 cm$^{-1}$. See the text for a discussion of this band and the nearby 1010 cm$^{-1}$ band (assigned to either $21^1$ or $33^135^1$).

[d]The ? marks an additional band with an uncertain assignment ($17_1$ or $26_135_138_1$).

[e]The +971, +1157, and +1185 cm$^{-1}$ bands have somewhat broader widths in the LIF excitation spectrum and are probably unresolved doublets. An assignment of both components is available only for the +1157 cm$^{-1}$ band ($17^1$ or $27^3$).

[f]The ? marks an unassigned band at 1340 cm−1.

(iv) Unexpectedly and contrary to the selection rules, we observed relatively strong excitation bands that we assigned to ''forbidden'' transitions, e.g., to $27^139^1$ (at $S_1 + 557$ cm$^{-1}$) and to $27^138^1$ (at $S_1 + 568$ cm$^{-1}$). These as-

TABLE II. $S_0$ state vibrational fundamentals of 1H-indazole.

| Vibrational mode | | Frequency of fundamental ($cm^{-1}$)[a] | | | | DF intensity[b] | IR intensity[c] | |
|---|---|---|---|---|---|---|---|---|
| | | DF | IR | MP2/6–31G* | Obs./Calc. | | Obs. | Calc. |
| $A'$ | 1 | | 3500/3523[d] | 3572 | 0.98 | ⋯ | m,s | 4.42 |
| | 2 | | 3104/3120[d] | 3294 | 0.94 | ⋯ | w,w | 3.48 |
| | 3 | | 3080 | 3244 | 0.95 | ⋯ | m | 14.38 |
| | 4 | | 3067 | 3235 | 0.95 | ⋯ | m | 19.09 |
| | 5 | | 3059 | 3225 | 0.95 | ⋯ | m | 1.56 |
| | 6 | | 3033 | 3218 | 0.94 | | w | 0.34 |
| | 7 | | 1626 | 1702 | 0.96 | ?[e] | m | 7.79 |
| | 8 | | 1586 | 1650 | 0.96 | ?[e] | w | 0.32 |
| | 9 | | 1503 | 1566 | 0.96 | ?[e] | m | 12.35 |
| | 10 | | 1480 | 1542 | 0.96 | ?[e] | w | 2.84 |
| | 11 | 1433 | 1430 | 1515 | 0.95 | w | w | 1.79 |
| | 12 | 1362 | 1360 | 1463 | 0.93 | m | m | 20.41 |
| | 13 | 1349 | 1347 | 1421 | 0.95 | s | m | 21.78 |
| | 14 | 1318 | 1316 | 1372 | 0.96 | s | vw | 2.22 |
| | 15 | 1269 | 1266 | 1318 | 0.96 | w | w | 3.40 |
| | 16 | 1245 | 1243 | 1284 | 0.97 | ⋯ | w | 10.62 |
| | 17 | 1205 | 1203 | 1263 | 0.95 | ⋯ | w | 5.26 |
| | 18 | ⋯ | 1149 | 1207 | 0.95 | ?[e] | w | 4.01 |
| | 19 | 1125 | 1124 | 1168 | 0.96 | ⋯ | w | 1.27 |
| | 20 | 1080 | 1078 | 1146 | 0.94 | vs | w | 9.46 |
| | 21 | 1010 | 1007 | 1048 | 0.95 | m | w | 5.78 |
| | 22 | 938 | 937 | 958 | 0.98 | m | s | 30.56 |
| | 23 | 900 | 903 | 912 | 0.99 | ⋯ | w | 1.78 |
| | 24 | 766 | 765 | 788 | 0.97 | vs | w | 6.47 |
| | 25 | 618 | 618 | 630 | 0.98 | vs | vw | 1.27 |
| | 26 | 534 | ⋯ | 548 | 0.97 | w | ⋯ | 0.23 |
| | 27 | 393 | 397 | 400 | 0.98 | w | vw | 1.25 |
| $A''$ | 28 | ⋯ | ⋯ | 879 | ⋯ | ⋯ | ⋯ | 0.03 |
| | 29 | 848 | 850 | 861 | 0.99 | | s | 0.50 |
| | 30 | 832 | 833 | 806 | 1.03 | ⋯ | s | 0.17 |
| | 31 | ⋯ | ⋯ | 801 | ⋯ | ⋯ | | 44.81 |
| | 32 | 741 | 739 | 720 | 1.03 | ⋯ | vs | 54.87 |
| | 33 | 656 | 652 | 661 | 0.99 | ⋯ | s | 37.93 |
| | 34 | 567 | 565 | 580 | 0.98 | ⋯ | vw | 6.02 |
| | 35 | 424 | 418 | 443 | 0.96 | ⋯ | w | 9.78 |
| | 36 | 406 | 405 | 403 | 1.01 | ⋯ | s | 21.65 |
| | 37 | 415 | 415 | 371 | 1.12 | ⋯ | s | 37.68 |
| | 38 | 247 | ⋯ | 241 | 1.02 | ⋯ | | 0.12 |
| | 39 | 205 | ⋯ | 206 | 1.00 | | | 1.01 |

[a]DF data and MF2/6–31G* data of this work, IR data from Ref. 5.
[b]Relative intensity of the DF band $0_0^0$ excitation.
[c]The A′ modes give rise to A−, B−, or A+B− type IR absorption bands, while the $A''$ modes give rise to *C*-type bands.
[d]Two alternative assignments had been proposed for $\nu_1$ and $\nu_2$ (Ref. 5).
[e]The ? marks a mode for which the observation in the DF spectrum after $0_0^0$ excitation remained uncertain due to overlapping other bands at the same frequency.
[f]The observed levels at 848 and 833 $cm^{-1}$ were attributed to $\nu_{29}$ and $\nu_{30}$, although assignments to $\nu_{31}$ or $\nu_{28}$ could not be excluded.

signments were the only ones consistent with the DF spectra from the respective $S_1$ levels, although they have $A''$ vibrational symmetry and the observed bands are therefore formally forbidden. These transitions will be considered separately below.

(v) A series of excitation bands may lead to excited state Fermi multiplets.

(vi) Assignments of several excitation bands (Table I) remained somewhat tentative due to the lack of suitable combinations that could be used to test the conclusions.

(vii) Excitation in several weak bands (labeled in Fig. 4 by asterisks) resulted in DF spectra with very broad features (spectral widths of $\approx 150-250\ cm^{-1}$). These were attributed to indazole–water clusters (see below).

### D. $S_1 \rightarrow S_0$ dispersed fluorescence spectra

DF spectra enabled us to find vibrational mode assignments for the indazole molecule in the $S_0$ state and in the $S_1$ state. The frequencies of the $S_0$ vibrational fundamentals that we extracted from the DF spectra are listed in Table II. This table furthermore lists the frequencies from the IR absorption spectra of indazole vapor of Cané *et al.*[5] and the frequencies

TABLE III. $S_1$ state vibrational fundamentals of 1H-indazole.

| Vibrational mode | | Frequency of fundamental ($cm^{-1}$)[a,b] Obs. | CIS/6–31G* | Obs./Calc. |
|---|---|---|---|---|
| $A'$ | 1 | ⋯ | 3906 | ⋯ |
| | 2 | | 3435 | |
| | 3 | | 3407 | |
| | 4 | | 3399 | |
| | 5 | | 3387 | |
| | 6 | | 3374 | |
| | 6 | | 1781 | |
| | 8 | | 1697 | |
| | 9 | | 1641 | |
| | 10 | | 1587 | |
| | 11 | | 1576 | |
| | 12 | | 1519 | |
| | 13 | | 1482 | |
| | 14 | | 1426 | |
| | 15 | 1263 | 1407 | 0.90 |
| | 16 | ⋯ | 1340 | ⋯ |
| | 17 | 1158 | 1281 | 0.90 |
| | 18 | ⋯ | 1255 | ⋯ |
| | 19 | 1040 | 1148 | 0.91 |
| | 20 | 946 | 1075 | 0.88 |
| | 21 | 889 | 980 | 0.91 |
| | 22 | 851 | 972 | 0.87 |
| | 23 | 813 | 958 | 0.85 |
| | 24 | 728 | 788 | 0.92 |
| | 25 | 586 | 645 | 0.91 |
| | 26 | 489 | 521 | 0.94 |
| | 27 | 385 | 426 | 0.91 |
| $A''$ | 28 | ⋯ | 983 | ⋯ |
| | 29 | ⋯ | 979 | ⋯ |
| | 30 | 809[c] | 818 | 0.99 |
| | 31 | ⋯ | 776 | ⋯ |
| | 32 | 593 | 751 | 0.79 |
| | 33 | 576 | 686 | 0.83 |
| | 34 | 487 | 615 | 0.79 |
| | 35 | 493 | 601 | 0.82 |
| | 36 | 281 | 453 | 0.62 |
| | 37 | 270 | 337 | 0.80 |
| | 38 | 182 | 219 | 0.83 |
| | 39 | 172 | 190 | 0.91 |

[a]Data from LIF excitation spectra and CIS/6–31G* data of this work.
[b]Only the lower-frequency modes ($\nu_{15}$–$\nu_{39}$) were assigned in the experimental excitation spectra because of the increasing spectral congestion toward the higher frequencies.
[c]The observed 809 $cm^{-1}$ level was attributed to $\nu_{30}$, although assignments to $\nu_{28}$, $\nu_{29}$, or $\nu_{31}$ could not be excluded.

predicted by the MP2/6-31G* calculations of the present work. The corresponding data for the $S_1$ state obtained from the excitation spectra and from the CIS/6-31G* calculations are compiled in Table III. Only the lower-frequency modes ($\nu_{15}$–$\nu_{39}$) of the $S_1$ state were assigned in the observed excitation spectra because of the increasing spectral congestion toward higher energies.

The DF spectrum of indazole observed after excitation in the $S_1 \leftarrow S_0$ origin band ($0_0^0$) is depicted in Fig. 5. In addition, Figs. 6(a)–6(d) display measured DF spectra obtained after excitation in different higher-frequency $S_1 \leftarrow S_0$ vibronic bands. The DF spectra from the higher-energy $S_1$ levels are shown in Fig. 6 in the order of increasing excitation in the $S_1$ state. The top trace in each panel reproduces the DF

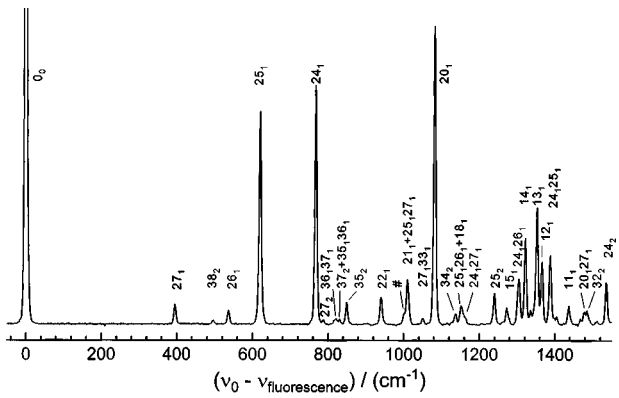


FIG. 5. The measured DF spectrum of indazole following excitation of the $S_1 \leftarrow S_0$ ($0_0^0$) origin (resolution: $\approx 7$ $cm^{-1}$). The # marks an unassigned band at 1000 $cm^{-1}$.

spectrum from the $S_1$ origin ($0^0$) for comparison. The strongest features in the DF spectra have been clipped to save space; assignments of these strongest bands are given as the $S_0$ ''counterparts'' of the respective $S_1$ modes in column 4 in Table I.

### 1. DF spectrum after excitation of the $S_1(0^0)$ origin level

Leaving aside the expected strong $0_0^0$ band, the DF spectrum from the $S_1$ electronic origin level (Fig. 5) was found to be dominated by $v=0 \rightarrow 1$ transitions to $S_0$ in-plane fundamentals (i.e., $v=1$ levels) and their combinations.

The strongest DF bands originating from the $S_1$ $0^0$ level were assigned to transitions to the $25_1$, $24_1$, and $20_1$ fundamentals in the $S_0$ state. These assignments were made in correspondence with those of the observed strong bands in the excitation spectrum (the somewhat complicated case of $20_1$ will be considered further below) and in accordance with the *ab-initio* frequency numbering. Transitions to the other $S_0$ in-plane fundamentals were found to be significantly weaker. The low-frequency $27_1$ and $26_1$ in-plane fundamentals were identified based on their calculated frequencies. Other fundamentals (and various combination bands) could be assigned with the help of the DF spectra from higher $S_1$ levels below. Four $S_0$ fundamentals ($23_1$, $19_1$, $17_1$, and $16_1$) were absent in the $0^0$ level DF trace; they were identified below in DF spectra from higher excitation levels. Apparently, the geometry change along these modes on the $S_1 \rightarrow S_0$ electronic transition is too small to produce significant $v=0 \rightarrow 1$ band intensities. The $18_1$ fundamental was not unambiguously distinguished because of overlapping DF bands to $25_1 26_1$ and $24_1 27_1$.

Bands involving $S_0$ fundamentals with frequencies of $\geqslant 1450$ $cm^{-1}$ ($\nu_1$–$\nu_{10}$) were weak and could not be distinguished as the DF spectrum became too congested toward higher $S_0$ vibrational energies. The weak DF bands to two quantum combinations and overtones of $S_0$ out-of-plane modes, which can be seen in Fig. 5, and ''forbidden'' transitions involving combinations of $27_1$ with out-of-plane

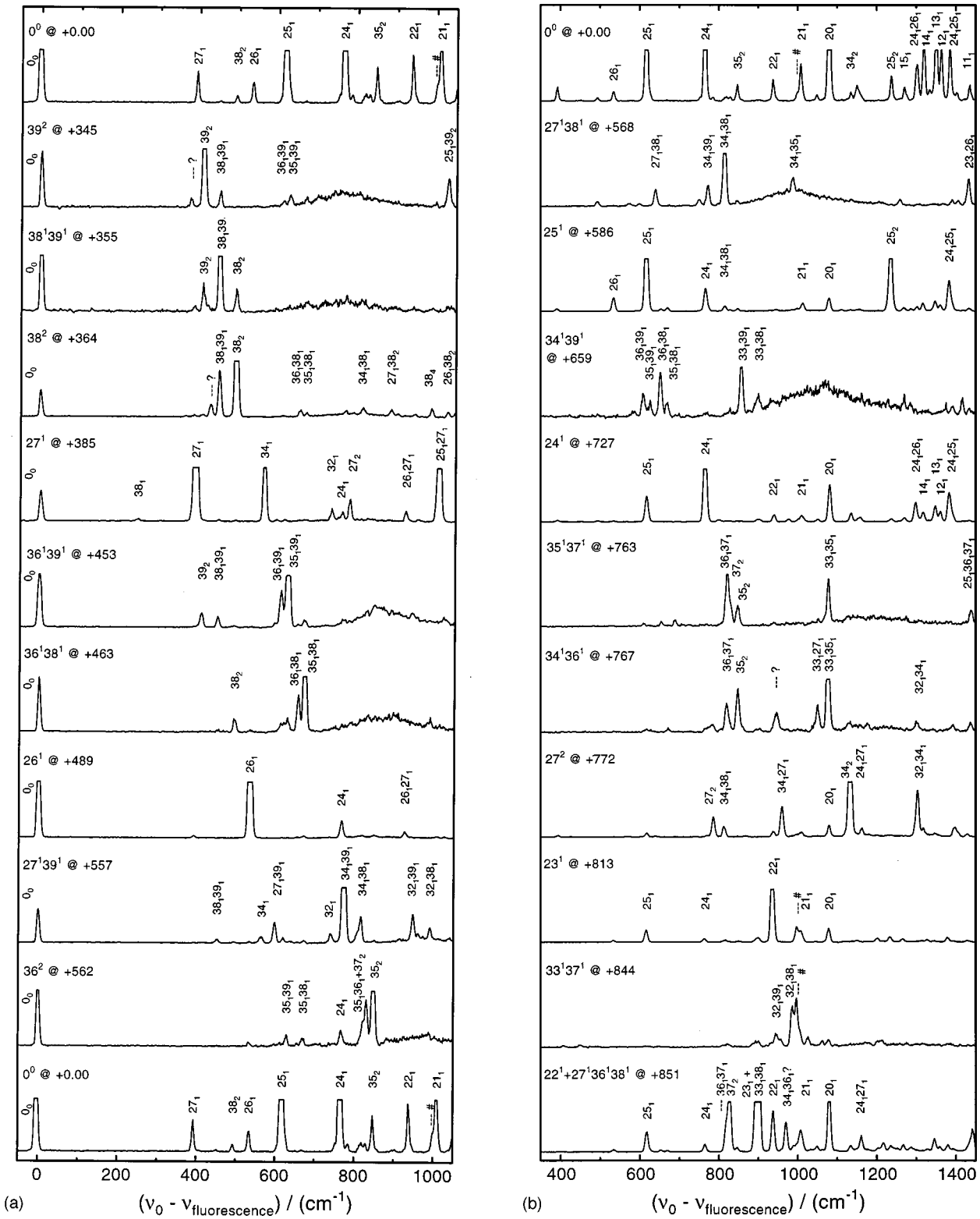


FIG. 6. Measured DF spectra of 1H-indazole from $S_1$ excited vibronic levels. Spectral resolution: $\approx 8\ \mathrm{cm}^{-1}$. The spectra in (a)–(d) are given in the order of increasing $S_1$ state excitation energies, labeled by the $S_1$ vibrational level and energy. Strong DF bands have been clipped to save space. One spectrum ($S_1 + 1111\ \mathrm{cm}^{-1}$) has been recorded with twice lower resolution. Question marks indicate unassigned bands or uncertain assignments.

modes (e.g., $27_1 33_1$ in Fig. 5), which were observed despite their $A''$ symmetry, will be considered below.

### 2. DF spectra after excitation of $S_1$ in-plane ($A'$) modes

The large number of DF spectra taken from higher-energy $S_1$ vibronic levels (Fig. 6) allowed us to ascertain the $S_0$ and the $S_1$ vibrational mode assignments. As noted, the observed band intensities provided strong arguments. In the following, we consider the respective vibrations and DF scans roughly in the order in which assignments could be made.

*a. The* $27_1$, $26_1$, $25_1$, $24_1$, $19_1$, *and* $15_1$ ($S_0$) *funda-*

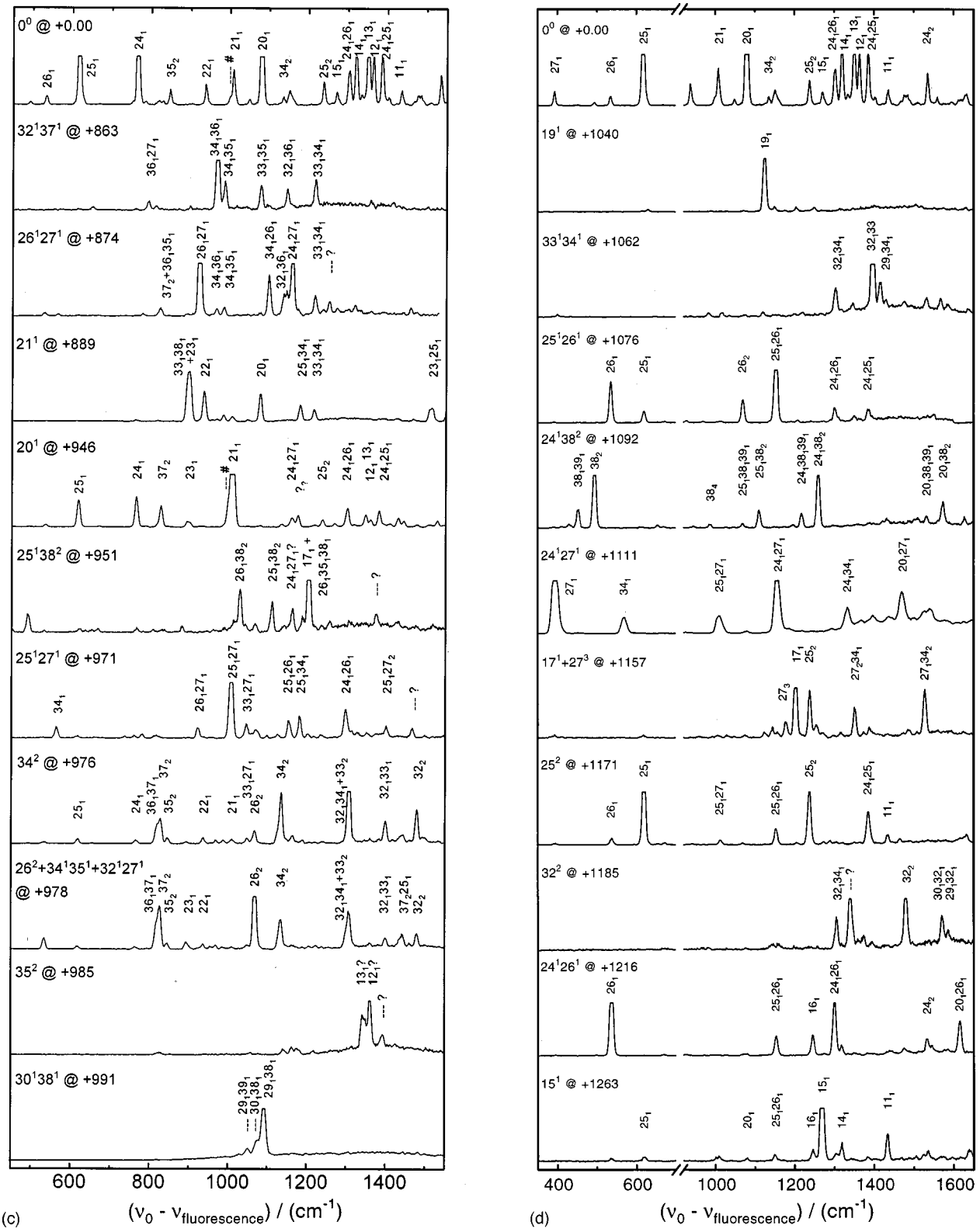


FIG. 6. (*Continued*)

*mentals:* The $S_0$ in-plane fundamentals $27_1$ to $24_1$, as well as $19_1$ and $15_1$, and their $S_1$ counterparts ($27^1$ to $24^1$, and $19^1$ and $15^1$, respectively) were identified from the strong $\Delta v = 0$ type bands observed in the DF spectra from these $S_1$ vibronic levels (see Fig. 6 and Table II). The calculated $S_0$ *ab-initio* frequencies and the respective experimental data are in good agreement. Assignments for the other $S_0$ in-plane fundamentals (considered in the following) did, however, turn out to be somewhat more complicated.

*b. The* $22_1$ ($S_0$) *fundamental:* The $22_1$ fundamental ($958\,\mathrm{cm}^{-1}$ in $S_0$) has been observed as a strong IR mode in the spectrum of Cané *et al.*[5] and it also had a high calculated

IR intensity. It was clearly visible in the DF spectra from the $S_1\ 0^0$ origin and from the $23^1$ level (at $S_1+813\,\mathrm{cm}^{-1}$). Thus, with our frequency numbering according to the *ab-initio* values, the $22_1$ $S_0$ fundamental has its $S_1$ ''counterpart'' in the $23^1$ level.

The complicated DF spectrum obtained after excitation to the $S_1+851\,\mathrm{cm}^{-1}$ level, nominally assigned as $22^1$ [Fig. 6(b)], suggests that this excitation leads to more than one $S_1$ level (which could be subject to a Fermi-type interaction). A plausible candidate for a coinciding second $S_1$ level is $27^136^138^1$. Two other combinations ($26^138^2$ and $34^138^2$) that would also be close in frequency were rejected because of the absence of combination bands involving the $38_2$ overtone in the DF spectrum.

*c. The* $23_1$ *and* $21_1$ ($S_0$) *fundamentals:* The frequencies of the $23_1$ and $21_1$ ($S_0$) fundamentals were calculated to be at 912 and $1048\,\mathrm{cm}^{-1}$, respectively. Experimentally observed $S_0$ bands in this range were at 900, 938, 1000, and $1010\,\mathrm{cm}^{-1}$. Their somewhat larger uncertainties ($\approx 5-10\,\mathrm{cm}^{-1}$) were due here to overlapping neighboring DF bands. The $938\,\mathrm{cm}^{-1}$ band was already assigned above to $22_1$.

We assigned the observed $900\,\mathrm{cm}^{-1}$ band to the $23_1$ ($S_0$) fundamental. It was found to dominate in the DF spectra following excitation to $22^1$ [at $S_1+851\,\mathrm{cm}^{-1}$; Fig. 6(b)] and $21^1$ [at $S_1+889\,\mathrm{cm}^{-1}$; Fig. 6(c)]. This $900\,\mathrm{cm}^{-1}$ band ($23_1$) was somewhat broader than other bands, suggesting that it might consist of two nearly coinciding bands (the second one may be $33_138_1$). The presence of the $23_1$ in-plane mode near $900\,\mathrm{cm}^{-1}$ was supported by the *ab-initio* predictions and by the observed IR band[5] at $903\,\mathrm{cm}^{-1}$.

The $1010\,\mathrm{cm}^{-1}$ band was assigned to the $21_1$ ($S_0$) fundamental. Its $S_1$ counterpart is mostly $20^1$ [as seen from the strong $1010\,\mathrm{cm}^{-1}$ DF band from $20^1$ at $S_1+946\,\mathrm{cm}^{-1}$ to $21_1$ in Fig. 6 (c)]. The $1010\,\mathrm{cm}^{-1}$ band appeared in the DF spectra in most cases, together with the $1000\,\mathrm{cm}^{-1}$ band. The $1010\,\mathrm{cm}^{-1}$ feature was stronger in the DF following excitation to the $S_1\ 0^0$ origin and to $S_1+851\,\mathrm{cm}^{-1}$ ($22^1$) and $S_1+946\,\mathrm{cm}^{-1}$ ($20^1$). In contrast, the $1000\,\mathrm{cm}^{-1}$ feature was stronger in the DF following excitation to $S_1+813\,\mathrm{cm}^{-1}$ ($23^1$) and $S_1+844\,\mathrm{cm}^{-1}$ ($33^137^1$). A further complication was that this $21_1$ fundamental and the $25_127_1$ combination have the same frequencies. We assumed that $25_127_1$ dominated over $21_1$ only in the DF spectrum following $25^127^1$ excitation (at $S_1+971\,\mathrm{cm}^{-1}$). The band at $1000\,\mathrm{cm}^{-1}$ [''#'' in Figs. 6(a) and 6(b)] remained unassigned. Its frequency does not match any identified out-of-plane mode combination. Although the IR measurements[5] showed three weak bands (at 997, 1007, and $1012\,\mathrm{cm}^{-1}$), our *ab-initio* calculations predicted only one in-plane fundamental ($21_1$) with a frequency near $1000\,\mathrm{cm}^{-1}$.

*d. The* $20_1$ ($S_0$) *fundamental:* By comparison of the band intensities in the DF spectrum from the $S_1$ origin (Fig. 5) and in the LIF excitation spectrum (Fig. 4), one might suppose that the strong $S_0$ band at $1080\,\mathrm{cm}^{-1}$ seen in the DF trace from $0^0$ corresponds to the strong band at $S_1+946\,\mathrm{cm}^{-1}$ in the excitation spectrum. In accordance with the frequency ordering, the DF signal at $1080\,\mathrm{cm}^{-1}$ ($S_0$) was assigned to $20_1$ and the $S_1+946\,\mathrm{cm}^{-1}$ excitation band was assigned to $20^1$. However, as already noted in the preceding paragraph, the DF scan from $20^1$ ($S_1+946\,\mathrm{cm}^{-1}$) showed that the $S_0$ counterpart of that mode is mostly $21_1$ (which was the strongest in the DF from $20^1$, but relatively weak in the DF from $S_1\ 0^0$). In contrast, the $20_1$ fundamental ($1080\,\mathrm{cm}^{-1}$ in $S_0$) appeared mostly in the DF spectra from $24^1$, $23^1$, and $22^1$ (at $S_1+727$, $S_1+813$, and $S_1+851\,\mathrm{cm}^{-1}$) and, less so, from $21^1$ (at $S_1+889\,\mathrm{cm}^{-1}$). Consequently, the $20_1$ ground state mode has its counterpart(s) in those $S_1$ modes, rather than in the $S_1+946\,\mathrm{cm}^{-1}$ mode ($20^1$).

*e. The* $18_1$, $17_1$, *and* $16_1$ ($S_0$) *fundamentals:* The frequency of the $18_1$ ($S_0$) mode remained ambiguous from our DF spectra because of overlap with the $25_126_1$, $24_127_1$, and $32_136_1$ combinations. However, the IR band at $1149\,\mathrm{cm}^{-1}$ was assigned to that mode. The $17_1$ mode ($1205\,\mathrm{cm}^{-1}$ in $S_0$) appeared only in the DF following excitation of the corresponding $17^1$ level (at $S_1+1157\,\mathrm{cm}^{-1}$). The $16_1$ mode ($1245\,\mathrm{cm}^{-1}$ in $S_0$) was assigned to a weak band on the red side of the $15_1$ band in the DF spectrum from the $15^1$ ($S_1$) level. The $15_1$ fundamental was identified above.

*f. Higher frequency in-plane fundamentals and combination modes:* The remaining higher-frequency $S_0$ in-plane fundamentals were difficult to identify in the DF spectra because of their weaker intensities and because of the increasing spectral congestion. Fortunately, the IR absorption data[5] allowed us to assign most of these modes by comparison with the *ab-initio* frequencies (see Table II). We note that excitation in several stronger $S_1 \leftarrow S_0$ bands produced DF spectra with patterns similar to those in the DF spectrum of $S_1\ 0^0$. For example, a distinctive quintet of bands (assigned to $24_126_1$, $14_1$, $13_1$, $12_1$, and $24_125_1$ of $S_0$) in the $1300-1400\,\mathrm{cm}^{-1}$ region appearing in the DF spectrum from $S_1\ 0^0$ was easily recognizable also in the DF spectra from $S_1$ $25^1$, $24^1$, $22^1$, and $20^1$ [Figs. 6(b) and 6(c)]. This effect was attributed to strong resonance fluorescence bands serving as pseudo-origins for originlike DF spectra.

Additional DF spectra originating from the $S_1$ overtone and combination levels of the in-plane modes were assignable in several cases because of their predictable band frequencies and clear DF band structures; some examples can be found in Fig. 6(d).

### 3. DF spectra after excitation of $S_1$ out-of-plane ($A''$) modes

Since the fundamental (i.e., $v=1$) vibrational levels of the out-of-plane ($A''$) modes in the $S_1$ state cannot be accessed from the $S_0$ vibrationless state ($A'$) because of the $A' \leftrightarrow A'$, $A'' \leftrightarrow A''$ selection rule for the transition, we could not directly observe the respective $S_0$ state $A''$ fundamentals in DF, as we did above for the $A'$ fundamentals. Hence, we deduced out-of-plane mode assignments from combination and overtone bands. DF bands from $S_1$ excited levels of $A'$ symmetry to $S_0$ state out-of-plane mode first overtones and two-quantum combinations with $A'$ symmetry were fully ''allowed'' by the symmetry selection rules.

*a. The* $39_1$ *and* $38_1$ ($S_0$) *modes:* The lowest-frequency $A''$ modes $\nu_{39}$ and $\nu_{38}$ were straightforward to assign by their overtone and combination bands. In the $S_1$ state, the $39^2$, the $38^139^1$, and the $38^2$ level were identified at $S_1+345$, $S_1$

+355, and $S_1+364\,cm^{-1}$. The DF spectra from these three nearly equally spaced $S_1$ levels showed the strongest features in the $S_0$ state at 410, 442, and 494 $cm^{-1}$ [see Fig. 6(a)]. This led to their assignments as ''allowed'' two quantum combinations of those out-of-plane modes ($39_2$, $38_1 39_1$, and $38_2$, respectively). The calculated *ab-initio* $S_0$ frequencies matched the experimental ones very nicely.

Excitation of $S_1$ levels containing the $38^2$ overtone in combination with one of the in-plane modes [see, e.g., $24^1 38^2$ at $S_1+1092\,cm^{-1}$; Fig. 6(d)] resulted in DF spectra showing in $S_0$ the $38_2$ overtone combined with an in-plane mode or the $38_1$ fundamental combined with another out-of-plane mode. The $38_2$ overtone was always accompanied by a 42 $cm^{-1}$ red-shifted satellite containing $38_1 39_1$.

*b. The* $36_1$ *and* $35_1$ ($S_0$) *modes:* Similar arguments applied to $\nu_{36}$ and $\nu_{35}$. The $\nu_{36}$ vibration was seen in the excitation spectrum in combinations with $\nu_{39}$ and $\nu_{38}$ ($36^1 39^1$ at $S_1+453\,cm^{-1}$ and $36^1 38^1$ at $S_1+463\,cm^{-1}$) and as first overtone ($36^2$ at $S_1+562\,cm^{-1}$). Excitation of those $S_1$ levels showed mostly respective DF combination bands containing $35_1$, accompanied by a 18 $cm^{-1}$ red-shifted band of the similar combination of $36_1$. Again, the $S_0$ *ab-initio* frequencies (or frequency combinations) matched the experimental ones. The $36^1$ ($S_1$) mode is mostly the ''counterpart'' of the $35_1$ ($S_0$) mode.

*c. The* $37_1$ ($S_0$) *mode:* The strong IR band at 415 $cm^{-1}$ has been assigned to the $37_1$ $S_0$ fundamental. The observed $S_0$ frequency has to be compared with the calculated one of 371 $cm^{-1}$, which implies a somewhat larger deviation than for the other modes. In the DF spectra, $\nu_{37}$ appeared in the $36_1 37_1$ combination and the $37_2$ overtone bands (both not completely resolved) following excitation to a series of $S_1$ levels (at $S_1+562$, $S_1+763$, $S_1+767$, $S_1+851$, $S_1+976$, and $S_1+978\,cm^{-1}$). There were also several very weak and poorly resolved bands in the region from 810 to 830 $cm^{-1}$ in the DF trace from the $S_1$ $0^0$ origin, which may be attributed to combinations and overtones involving $\nu_{37}$, among others (e.g., $36_2$, $34_1 38_1$, $36_1 37_1$, $37_2$, $36_1 35_1$; the $35_1 37_1$ combination was, however, not observed).

As seen from Fig. 2(a), $\nu_{37}$ has significant NH out-of-plane bending character. In the $S_1$ state, on the other hand, the NH out-of-plane bending motion is more distributed [see $\nu_{38}$, $\nu_{35}$, $\nu_{34}$, and $\nu_{33}$ in Fig. 2(b)]. This distributed character in $S_1$ is reflected by the DF spectra from those excited $S_1$ levels which contain DF bands to the $37_1$ level.

*d. The* $34_1$, $33_1$, *and* $32_1$ ($S_0$) *modes:* Several DF bands were assigned to overtones and combinations among $34_1$, $33_1$, and $32_1$ ($S_0$). The $\nu_{34}$ mode in the $S_1$ state is mostly the counterpart of $\nu_{33}$ in the $S_0$ state [see the DF trace from $34^2$ at $S_1+976\,cm^{-1}$; Fig. 6(c)].

*e. The* $31_1$, $30_1$, $29_1$, *and* $28_1$ ($S_0$) *modes:* The IR absorption bands at 833 and 850 $cm^{-1}$ (Ref. 5) were identified in the DF spectra after excitation at $S_1+991\,cm^{-1}$ ($30^1 38^1$) and $S_1+1185\,cm^{-1}$ ($32^2$). We labeled these DF bands as $30_1$ and $29_1$ for convenience, although $31_1$ or $28_1$ would also fit (see Table II). These vibrations are CH bending modes; more data would be needed to ascertain their assignments.

The IR bands observed[5] at 1047 and 1391 $cm^{-1}$ could be attributed to several $S_0$ state combinations, for example, $27_1 33_1$ (or $27_1 36_1 38_1$) and $32_1 33_1$, respectively. The IR band at 1579 $cm^{-1}$ could be tentatively assigned to $30_1 32_1$.

### E. Forbidden transitions

Transitions between ($S_1$) $A'$ and ($S_0$) $A''$ symmetry levels (and vice versa) contradict the $A' \leftrightarrow A'$, $A'' \leftrightarrow A''$ vibrational selection rules for the electronic transition. Nevertheless, the observed spectra were found to exhibit ''forbidden'' bands of this type, in the excitation scan and in DF, in connection with the $S_1$ state $\nu_{27}$ mode. They may formally gain intensity if the $S_1$ electronic state (which nominally is $A'$) contains some character of a higher-energy $A''$ electronic state.

A striking case was the DF trace from the $27^1$ excited state level [at $S_1+385\,cm^{-1}$; Fig. 6(a)]. That DF spectrum was seen to contain an unexpected band at 567 $cm^{-1}$ with an intensity of nearly 10% of that of the strongest band (which belongs to the $27_1$ $S_0$ level at 392 $cm^{-1}$). Guided by the IR data[5] and by the *ab-initio* predictions, the respective band was assigned to the $34_1$ ($S_0$) out-of-plane fundamental. Apart from this $34_1$ mode, the DF trace also showed very weak bands belonging to the $38_1$ and $32_1$ fundamentals. ''Forbidden'' bands were also observed in the excitation spectrum, where they were assigned to $27^1 39^1$ (at $S_1+557\,cm^{-1}$) and to $27^1 38^1$ (at $S_1+568\,cm^{-1}$). DF scans from those $27^1 39^1$ and $27^1 38^1$ levels produced corresponding ''forbidden'' bands to the $34_1 39_1$ and $34_1 38_1$ ($S_0$) combinations; the expected transitions to the $27_1 39_1$ and $27_1 38_1$ combinations formed much weaker bands. Combination bands involving $\nu_{27}$ and $\nu_{34}$ were also present in the DF from $27^2$ ($S_1+772\,cm^{-1}$) and $27^3$ ($S_1+1158\,cm^{-1}$).

Few DF bands remained for which we did not find proper assignments. These have been marked ''?'' in Fig. 6. It is possible in some cases that the excitation of indazole–water complexes under the assigned indazole monomer excitation bands or weak ''hot band'' excitation transitions of the monomer gave rise to some of the unassigned DF features.

### F. Indazole–water complexes

A number of DF spectra showed very broad ($\approx$150–250 $cm^{-1}$ wide) features. We attributed those spectra to indazole–water complexes. That conclusion was confirmed by the observation that the excitation bands giving broad DF were significantly stronger after loading a new indazole sample (with higher $H_2O$ impurity) into the sample vessel (compare Figs. 3 and 4). Figure 7 depicts a DF spectrum with such broad features. The upper panel shows a DF trace recorded after tuning the excitation dye laser to a weak $S_1 \leftarrow S_0$ band of the indazole–water complexes at 324 $cm^{-1}$ toward the blue of the electronic origin of the monomer. The dramatic difference between this DF spectrum of the complex and the DF spectrum of the indazole monomer becomes obvious by comparison with the monomer DF spectrum from the $S_1$ origin plotted in the lower panel of the figure.

Similar broad features were observed in some of the DF spectra described in the preceding section. An example was the DF trace from the $S_1+659\,cm^{-1}$ excitation band (assigned to $S_1$ $34^1 39^1$ of the monomer) in Fig. 6(b). In this and

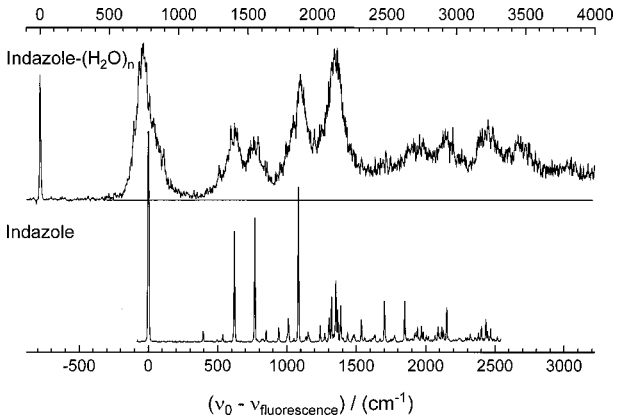


FIG. 7. The DF spectrum of indazole–water complexes showing strongly broadened ($\approx 150\ \mathrm{cm}^{-1}$) spectral features. The spectrum was observed after excitation of a weak $S_1$ band at $324\ \mathrm{cm}^{-1}$ blue from the electronic origin of the free indazole monomer (upper trace). The $S_1$ origin DF spectrum of the monomer is shown for a comparison in the lower trace.

other spectra, broad features were observed as the background under the sharp, structured DF bands of the monomer. We attribute those broad DF features to accidental coincidences of some very weak excitation bands of the indazole–water complexes with stronger monomer excitation bands. Apparently, those LIF excitation bands that gave rise to broad, unstructured DF features led to vibrationally highly excited $S_1$ indazole–water complexes.

Broad DF spectra were not observed when the excitation dye laser was set to any of the bands (see Fig. 3) toward the red of the $S_1$ origin of the free monomer. Those excitation bands gave sharp and structured DF, but they now exhibited many very low-frequency bands typical for intermolecular vibrations within the complexes. The structured, sharp character persisted partially also in the DF from excitation of a few very weak bands blue from origin of the monomer (for example, at $S_1+443$ and $S_1+539\ \mathrm{cm}^{-1}$).

## IV. DISCUSSION

### A. Franck–Condon allowed bands in the excitation and DF spectra

The observed fluorescence excitation and dispersed fluorescence $S_1 \leftrightarrow S_0$ electronic spectra of indazole were seen to exhibit strong vibrational origin bands and relatively short progressions of a number of in-plane vibrational modes. The structure of the spectra resembled that of other arenes, for example, anthracene (see, e.g., Ref. 16). This indicates that the difference between the excited and ground state geometries is rather small. Accordingly, the detected $v=1$ levels (fundamentals) of the in-plane vibrational modes were assigned based on the comparison with the *ab-initio* $S_0$ (and $S_1$) vibrational frequency values and based on the dominating strong bands in the $\Delta v=0$ regions in the DF spectra. Strong $v=1\rightarrow 1$ DF bands resulted because of the small difference between the $S_1$ and $S_0$ electronic states. The observed IR absorption bands[5] provided additional support.

Larger discrepancies between the calculated and measured $S_1$ state frequencies complicated the $S_1$ mode assignments, except for the identification of the strongest $S_1 \leftarrow S_0$ excitation bands, associated with the in-plane vibrations. However, the calculated normal modes (Fig. 2) helped to identify corresponding ''pairs'' of $S_1$ and $S_0$ modes and ascertain correspondences between calculated and measured $S_1$ state modes in other cases. Similarities between corresponding ground and excited state normal mode shapes gave rise to qualitatively predictable band intensities in the DF spectra.

### B. Bands allowed by the Dushinsky effect

A number of weaker bands appearing in the excitation spectrum (and to a lesser extent in the $S_1$ origin band DF spectrum) were identified as first overtones and two-quantum combinations of $S_1$ out-of-plane modes. Transitions to these $A'$ symmetry overtone or combination levels of the $A''$ modes were Franck–Condon allowed; they gain intensities through changes of the vibrational frequencies upon electronic transition.

Other bands can acquire intensities because of the differences between the ground and excited state normal modes (Dushinsky effect).[15] These transitions are limited only by symmetry restrictions. The Dushinsky effect is a fairly ordinary effect for aromatic molecules (see, e.g., Ref. 17). A number of vibronic bands in the indazole DF spectra did reflect that effect for in-plane and for out-of-plane modes. We point here to the case of $\nu_{20}$: The $20_0$ ($S_0$) level was seen to light up in the DF from several $S_1$ modes, in particular, $24^1$, $23^1$, and $22^1$. We saw that the $20^1$ mode was not simply the $S_1$ ''counterpart'' of $20_0$ ($S_0$), although that appeared from a first glance at the strongest bands in the excitation and in the $S_1$ origin DF spectra. Another striking case was the $\nu_{37}$ (NH out-of-plane bending) vibration in the $S_0$ state versus the corresponding vibrations in the $S_1$ state, where the NH out-of-plane character was seen to be distributed between several other modes, according to the DF spectra and according to the calculated normal mode displacements. As shown by these examples, this apparent ''mode mixing'' in the spectra can be qualitatively examined by comparing the excited and ground state vibrational modes (Fig. 2). The strongest $v=1\rightarrow v'=1$ transitions occur between modes with similar shapes in $S_0$ and $S_1$. A change of the mode number upon electronic transition ($\Delta v=+1$, $\Delta v'=-1$ vibrational band type) may arise for the reason that two modes with similar character do not necessarily have the same frequency numbers in the two electronic states.

The $S_1$ and $S_0$ mode shapes and the geometry change on excitation from *ab-initio* results can be used for a quantitative evaluation of the elements of the Dushinsky matrix for in-plane and out-of-plane modes and the displacement factors along the in-plane normal modes. The results may then be employed (see, e.g., Refs. 17 and 18) to simulate the excitation and DF spectra for a comparison with the experimental spectra. Work in these directions is underway.[12]

### C. Fermi resonances

Possible excited state Fermi-type resonances (anharmonic coupling) could be identified by common bands appearing in the DF spectra from the multiplet components. One example for a probable coupling is the set of $34^2$, $26^2$,

and $34^1 35^1$ (at $S_1+976$ and $S_1+978\,\mathrm{cm}^{-1}$), another one the pair of $35^1 37^1$ and $34^1 36^1$ (at $S_1+763$ and $S_1+767\,\mathrm{cm}^{-1}$). The somewhat larger widths of the bands at $S_1+971$, $S_1+1157$, and $S_1+1185\,\mathrm{cm}^{-1}$ suggests that these too could be unresolved doublets, although only for the band at $S_1+1157\,\mathrm{cm}^{-1}$ could we tentatively identify the two states ($17^1$ and $27^3$). Accidental overlaps of bands could, however, not be excluded. Ground state interactions could not be unambiguously identified because of the limited spectral resolution. One possible candidate for an $S_0$ doublet would be the $23_1$, $33_1 38_1$ pair.

### D. Forbidden bands

The vibrational selection rules (within the Condon approximation) governing the indazole $S_1 \leftrightarrow S_0$ spectrum are $A' \leftrightarrow A'$, $A'' \leftrightarrow A''$, since the ground and excited electronic states are both $A'$. Within the harmonic approximation and the planarity assumption for the electronic states, the in-plane and out-of-plane modes in the ground and in the excited state of the molecule should not mix with each other. This was generally found to be the case, i.e., excitation into $A'$ modes, and their combinations in $S_1$ resulted in $A'$ modes dominating in the DF and, likewise, excitation into $A''$ overtones or combinations in $S_1$ resulted in $A''$ overtones and combinations in the DF.

''Forbidden'' transitions violating these vibrational selection rules did, however, seem to appear in the indazole spectrum according to our assignments. In the excitation spectrum, assuming that the assignments are correct, they seemed to involve combination bands of the $27^1$ in-plane $S_1$ mode with the $39^1$ and $38^1$ out-of-plane modes. Likewise, similar ''forbidden'' bands appeared in emission (DF) from the $27^1$ and $27^2$ levels and from combination levels of $27^1$ with other in-plane or out-of-plane modes. For example, the DF spectrum from $S_1$ $27^1$ contained $v=1 \rightarrow v'=1$ bands to several ground state out-of-plane fundamentals, the strongest one leading to the $34_1$ ($S_0$) out-of-plane fundamental [Fig. 6(a)].

The $\nu_{27}$ mode is the lowest- frequency in-plane vibration and we are rather confident that the levels assigned as $27_1$ and $27^1$ really do belong to that in-plane mode by a number of arguments. We accepted the $S_0$ state mode assignments from the IR investigation[5] for our analysis, noting again that the corresponding IR frequencies, our DF frequency data, and our *ab-initio* results for the $S_0$ state are in excellent agreement (cf. Table II). The assignment of $27^1$ in the $S_1$ state was supported on these grounds by the observation of the $27_1$ $S_0$ state counterpart of that mode as the strongest band in its DF. The out-of-plane nature of the assigned $S_0$ state $37_1$, $36_1$, and $35_1$ fundamentals, which have similar frequencies compared with $27_1$, was demonstrated by their $C$-type IR band structures[5] (the $27_1$ IR band type[5] was less certain). In our spectra, the $36_1$ and $35_1$ modes were identified based on the $36^1 39^1$ and $36^1 38^1$ DF. No room seems to be left for another out-of-plane mode with the same frequency ($385\,\mathrm{cm}^{-1}$) coinciding with the $27^1$ level.

Anharmonic coupling of $\nu_{27}$ in the $S_1$ state with another mode can mix only vibrational states of the same symmetry. Perturbing levels would have to be very closely spaced ($<5\,\mathrm{cm}^{-1}$). Coriolis-type (rotational–vibrational) coupling, which, in principle, can mix $A'$ and $A''$ modes is likely to be small (anharmonic and Coriolis effects are usually more important in floppy molecules with large-amplitude motions). Hence, one very likely has to look for a different mechanism by which those ''forbidden'' bands gain intensity.

A remaining possibility is vibronic coupling of the $S_1$ state (or the $S_0$ state) with another electronic state of $A''$ symmetry. The Herzberg–Teller effect[19,20] is usually invoked to explain the appearance of Franck–Condon forbidden $v=1 \leftarrow 0$ excitation and $v=0 \rightarrow 1$ emission transitions to nontotally symmetric excited state modes (see, e.g., Ref. 21). The Herzberg–Teller effect implies that the electronic transition dipole moment depends on the nuclear displacments along one or more of the out-of-plane normal mode coordinates. In the indazole excitation spectrum, however, we saw little evidence for strong $v=1 \leftarrow 0$ bands to excited out-of-plane fundamentals. A normal Herzberg–Teller mechanism therefore seems to be small in the indazole case. An option that should be of interest for further investigation is that the $\nu_{27}$ mode is involved directly or indirectly in vibronic coupling with an electronic state of $A''$ symmetry. A probable candidate would be an $n\pi^*$ electronic state obtained by promotion of a lone pair electron of one of the N atoms to the $\pi^*$ moiety. The CIS/6-31G* calculation predicts the $S_3$ state to be the lowest one with out-of-plane symmetry. Due to the weakness of the corresponding electronic transition it is likely masked by the strong $^1B_b$ state of in-plane symmetry observed at around $48\,000\,\mathrm{cm}^{-1}$ in the solution absorption spectrum.[1] Vibronic coupling involving the $27^1$ mode should on the other hand occur only between vibronic states with the same vibronic symmetry. In our case, however, the vibronic symmetry of the $27^1$ level of $S_1$ is $A'=A' \oplus A'$, different from the $A''$ symmetry of the $n\pi^*$ state. A vibronic activity of an out-of-plane mode seems to be required. This might imply a dependence of the transition dipole moment on the nuclear displacements in $S_1$ along the $\nu_{27}$ mode *and* one of the out-of-plane modes ($\nu_{39}$ and $\nu_{38}$ in particular). A vibronic coupling of the ground electronic state with the $n\pi^*$ state could also be invoked, although this possibility appears less likely by the large energy gap. In any case, the apparent mixing of in-plane and out-of-plane symmetry on the electronic transition seems to require a more sophisticated explanation.

A further confirmation of the proposed vibrational assignments could be achieved by an investigation of the 1D-indazole isotopomer. Also, a rotationally resolved excitation spectrum providing the direction of the $27^1$ vibronic transition dipole moment might help to solve the remaining puzzle.

### E. Indazole–water complexes

The spectra and dynamics of the observed indazole–water complexes are of great interest from a variety of standpoints. However, mass selective detection would be needed to identify the carrier(s) of the spectra and to unravel the structure and dynamics. While it is certain that the broad, unstructured DF is related to indazole–water complexes, it

remains to be seen whether only a single indazole $(H_2O)_1$ complex, several isomers of that complex, or perhaps also complexes with a number of $H_2O$ units are involved. A more detailed analysis of the spectra is the subject of our ongoing research.[12]

## V. CONCLUSIONS AND OUTLOOK

We have analyzed the $S_1 \leftarrow S_0$ vibronic excitation spectrum and the DF spectra from a large number of $S_1$ state vibronic bands of 1H-indazole. Characteristic intensity patterns in the DF spectra enabled us to distinguish the molecule's in-plane and out-of-plane modes and establish the correspondences between excited and ground state modes. In the $S_0$ electronic state, we assigned 25 (of 27) in-plane and 10 (of 12) out-of-plane vibrations by comparison with MP2/6-31G* frequency calculations and with the gas-phase IR absorption data of Cané *et al.*[5] The measured $S_0$ vibrational frequencies up to $1400\,cm^{-1}$ matched the calculated unscaled MP2/6-31G* frequencies to within 5% (exept for the NH bending modes, where the observed frequency was 12% higher). Remaining ambiguities of the assignments were discussed. In the $S_1$ state, we assigned 11 in-plane and 8 out-of-plane modes by comparison with CIS/6-31G* frequency calculations and by the correspondences between excited and ground state vibrations. The calculated CIS/6-31G* frequencies were overestimated on average by about 20%, and the observed-to-calculated frequency ratio was found to vary significantly from mode to mode.

A harmonic normal mode treatment was seen to be sufficient for assigning the observed vibrational modes. However, in order to explain the occurrence of overtone and combination bands or to describe observed intensities, mode mixing induced by the geometry change on the electronic transition (Dushinsky effect) and anharmonic interactions (Fermi-type resonances) have to be taken into account. Forthcoming work will be devoted to a comparison of observed band intensities with theoretical simulations based on mode mixing coefficients (elements of the Dushinsky matrix) and displacement factors extracted from the *ab-initio* results.

The observation of symmetry forbidden bands in several spectra was explained by vibronic coupling of the $S_1$ (or $S_0$) state to a higher $n\pi^*$-type electronic state with $A''$ symmetry.

The knowledge of the vibrational structure of 1H-indazole should be helpful for an elucidation of the 2H-tautomer. A detection of both tautomers would open a way for a spectroscopic probing of the tautomerization reaction (unimolecular proton transfer) in this molecule. A specific preparation will be needed to reach significant concentrations of 2H-indazole, which is predicted at an energy of $\approx 1300\,cm^{-1}$ above the 1H species. Furthermore, results of this work may be used for a reanalysis of the solid state IR and UV spectra, aiming at an elucidation of the perturbations of the indazole vibrational structure by the surroundings. The matrix environment is expected to affect mostly the NH motion and other out-of-plane modes. Eventually, a determination of the molecular parameters and the dynamics of the observed indazole–water complexes would be of considerable interest. Indazole–water may provide a nice example of a doubly hydrogen bonded complex through a five-membered ring, playing a role in biomolecules.

## ACKNOWLEDGMENTS

This work has been supported by the Fonds der Chemischen Industrie. The *ab-initio* frequency calculations were made on a CRAY supercomputer of the Conrad-Zuse-Zentrum für Informationstechnik in Berlin. E. J. thanks the Alexander von Humboldt Foundation for a research stipend and thanks Jan Roggenbuck for the help with the *ab-initio* calculations.

[1] H.-U. Schütt and H. Zimmermann, Ber. Bunsenges. Phys. Chem. **67**, 54 (1963).
[2] J. P. Byrne and I. G. Ross, Aust. J. Chem. **24**, 1107 (1971).
[3] B. Velino, E. Cané, A. Trombetti, G. Corbelli, F. Zerbetto, and W. Caminati, J. Mol. Spectrosc. **155**, 1 (1992).
[4] A. Bigotto and C. Zerbo, Spectrosc. Lett. **23**, 65 (1990).
[5] E. Cané, P. Palmieri, R. Tarroni, and A. Trombetti, J. Chem. Soc., Faraday Trans. **89**, 4005 (1993).
[6] E. Cané, A. Trombetti, B. Velino, and W. Caminati, J. Mol. Spectrosc. **155**, 307 (1992).
[7] G. Berden, W. L. Meerts, and E. Jalviste, J. Chem. Phys. **103**, 9596 (1995).
[8] J. Catalán, J. L. G. de Paz, and J. Elguero, J. Chem. Soc., Perkin Trans. 2 **1996**, 57; **1996**, 1027.
[9] G. A. Bickel, D. R. Demmer, E. A. Outhouse, and S. C. Wallace, J. Chem. Phys. **91**, 6013 (1989).
[10] E. Jalviste and A. Treshchalov, Chem. Phys. **172**, 325 (1993).
[11] W. Roth, C. Jacoby, A. Westphal, and M. Schmitt, J. Phys. Chem. A **102**, 3048 (1998).
[12] E. Jalviste and F. Temps (unpublished).
[13] GAUSSIAN 94, Revision D2, M. J. Frisch, G. W. Trucks, H. B. Schlegel *et al.* (Gaussian, Inc., Pittsburgh, PA, 1995).
[14] L. S. Slater and P. R. Callis, J. Phys. Chem. **99**, 8572 (1995).
[15] W. L. Smith, J. Mol. Spectrosc. **176**, 95 (1996); **187**, 6 (1998).
[16] W. R. Lambert, P. M. Felker, J. A. Syage, and A. H. Zewail, J. Chem. Phys. **81**, 2195 (1984).
[17] F. Negri and M. Z. Zgierski, J. Chem. Phys. **104**, 3486 (1996).
[18] P. R. Callis, J. T. Vivian, and L. S. Slater, Chem. Phys. Lett. **244**, 53 (1995).
[19] G. Fischer, *Vibronic Coupling* (Academic, London, 1984).
[20] J. M. Hollas, *High Resolution Spectroscopy* (Wiley, Chichester, 1998).
[21] S. M. Beck, D. E. Powers, J. B. Hopkins, and R. E. Smalley, J. Chem. Phys. **73**, 2019 (1980); **74**, 43 (1981).